

Research Article

Nonlinear Resonance of Cavities Filled with Bubbly Liquids: A Numerical Study with Application to the Enhancement of the Frequency Mixing Effect

María Teresa Tejedor Sastre  and Christian Vanhille 

Universidad Rey Juan Carlos, Tulipán, s/n. 28933 Móstoles, Madrid, Spain

Correspondence should be addressed to Christian Vanhille; christian.vanhille@urjc.es

Received 20 June 2018; Revised 16 October 2018; Accepted 8 November 2018; Published 6 December 2018

Academic Editor: Konstantin Avramov

Copyright © 2018 María Teresa Tejedor Sastre and Christian Vanhille. This is an open access article distributed under the Creative Commons Attribution License, which permits unrestricted use, distribution, and reproduction in any medium, provided the original work is properly cited.

This paper studies the nonlinear resonance of a cavity filled with a nonlinear biphasic medium made of a liquid and gas bubbles at a frequency generated by nonlinear frequency mixing. The analysis is performed through numerical simulations by mixing two source signals of frequencies well below the bubble resonance. The finite-volume and finite-difference based model developed in the time domain simulates the nonlinear interaction of ultrasound and bubble dynamics via the resolution of a differential system formed by the wave and Rayleigh–Plesset equations. Some numerical results, consistent with the literature, validate our procedure. Other results reveal the existence of a frequency shift of the cavity resonance at the difference-frequency component, which rises with pressure amplitude and evidences the global changes undergone by the bubbly medium under finite amplitudes. Finally, this work shows the enhancement of the amplitude of the difference-frequency component generated by parametric excitation using the nonlinear resonance shift, which is more pronounced when the second primary frequency is constant, the first one is varied to match the nonlinear resonance, and both have the same amplitude.

1. Introduction

Adding bubbles to a liquid modifies its acoustic properties [1–5]. The nonlinear parameter increases by several orders of magnitude. The sound speed, attenuation coefficient, compressibility, and nonlinear parameter acquire dispersive dependence on bubble resonance. The nonlinear interaction of ultrasound and bubble oscillations must be understood to take advantage of these properties in different applied frameworks such as sonochemistry [6], medicine [7], and others [8, 9]. Lauterborn, in [10], studies the nonlinear behavior of a single bubble in an acoustic field to analyze the effect of the pressure amplitude on the bubble resonance and concludes that a shift of the bubble resonance exists and is dependent on pressure amplitude.

The nonlinearity of the medium is responsible for the generation of harmonics from the fundamental frequency and generates combinations of frequencies by nonlinear frequency mixing (sum frequency and difference

frequency) when several ultrasonic signals travel through the medium [11]. These effects have multiple applications. Medical imaging can be generated from higher harmonic components [12]. Underwater exploration or transmission and nondestructive testing are fields where the difference-frequency signal has a huge interest because of its low attenuation, good directivity, and high penetration [13, 14]. Characterization and detection of bubbles are also attractive applications of the frequency mixing phenomenon [15–18].

Several studies based on linear models have been performed to understand the behavior of ultrasonic waves in bubbly liquids inside a cavity [19–21]. Omta studied the behavior of a bubbly liquid cloud in [22] showing that the nonlinear response emitted from the cloud, much lower than the bubble resonance, is determined mainly its total gas content. Other studies that analyze the behavior of standing ultrasonic waves are based on nonlinear models [23, 24]. In those papers, both the sound speed and the resonance

frequencies are calculated without taking into account the amplitude of the waves [2, 3]. In this paper, we aim at showing that the pressure amplitude of the signal changes the resonance of the cavity (and the sound speed).

The dependence of the resonance frequency on drive amplitude has been observed in solids, for which the nonlinear features of ultrasound are used in areas as damage diagnostics in materials [25], granular media and dynamic earthquake triggering [26], and fluids in closed tubes of variable cross section [27]. Omta also analyzed in [22] the signal emitted from a bubbly liquid cloud as a function of the amplitude of the acoustic perturbation, concluding that the frequency of this signal undergoes a variation that is amplitude dependent. Up to our knowledge, that paper, and more specifically its Figures 4–6, was the very first demonstration of the shift of the resonance of a bubbly cloud with pressure amplitude. Matsumoto and Yoshizawa, in [28], also detected the shift with pressure amplitude of the resonance of a cluster containing a bubbly liquid. This effect has also been studied in bubbly liquids for a resonance frequency associated to the multiple scattering of bubbles that changes as a function of the amplitude of an incident Gaussian pulse [29].

The objective of this work is to study the variation with pressure amplitude of the resonance of a one-dimensional resonator filled with a fluid made of a liquid and gas bubbles when working at nonlinear regime by mixing two finite-amplitude continuous excitation signals. Frequencies well below the bubble resonance are used to take advantage of the nonlinearity of the dispersive medium with a relative low attenuation.

In Section 2, we present the physical problem and the corresponding mathematical model used in this work. Several numerical experiments performed by varying the amplitude at the source are shown in Section 3. They allow us to observe the nonlinear resonance phenomenon of the cavity at the difference-frequency component generated by nonlinear frequency mixing. This resonance frequency shift is used to maximize its amplitude. Similarities with classic results are also commented. Section 4 gives the conclusions of this work.

2. Materials and Methods

We consider a one-dimensional cavity of length L filled with a mixture of water and air bubbles. Under the Rayleigh–Plesset approximation, we suppose that, among others, the bubbles are spherical and have the same size. We also assume that they are evenly distributed in the liquid. The model assumes that bubbles are the only source of attenuation, dispersion, and nonlinearity. The buoyancy and Bjerknes and viscous drag forces are not considered in this work. The interaction between the acoustic pressure $p(x, t)$ and the volume variation of the bubbles $v(x, t) = V(x, t) - v_{0g}$ is modeled by the wave equation, Equation (1), and a Rayleigh–Plesset equation, Equation (2) [3, 30], where x is the one-dimensional space coordinate, t is the time, V is the current volume of the bubble, and $v_{0g} = 4/3\pi R_{0g}^3$ is the initial bubble volume, with R_{0g} as the initial radius.

$$\frac{\partial^2 p}{\partial x^2} - \frac{1}{c_{0l}^2} \frac{\partial^2 p}{\partial t^2} = -\rho_{0l} N_g \frac{\partial^2 v}{\partial t^2}, \quad (1)$$

$$0 < x < L, \quad 0 < t < T_t,$$

$$\frac{\partial^2 v}{\partial t^2} + \delta \omega_{0g} \frac{\partial v}{\partial t} + \omega_{0g}^2 v + \eta p = av^2 + b \left(2v \frac{\partial^2 v}{\partial t^2} + \left(\frac{\partial v}{\partial t} \right)^2 \right), \quad (2)$$

$$0 \leq x \leq L, \quad 0 < t < T_t.$$

In Equation (1), c_{0l} and ρ_{0l} are the sound speed and the density at the equilibrium state of the liquid. N_g is the density of bubbles, i.e., the bubble number per m^3 . In Equation (2), $\delta = 4\gamma_l/\omega_{0g}R_{0g}^2$ is the viscous damping coefficient of the bubbly fluid, in which γ_l is the cinematic viscosity of the liquid and $\omega_{0g} = \sqrt{3\gamma_g p_{0g}/\rho_{0g}R_{0g}^2}$ is the resonance frequency of the bubbles, where γ_g is the specific heats ratio of the gas, $p_{0g} = \rho_{0g}c_{0g}^2/\gamma_g$ is its atmospheric pressure, and ρ_{0g} and c_{0g} are the density and sound speed at the equilibrium state of the gas. The parameter $\eta = 4\pi R_{0g}/\rho_{0l}$ and the nonlinear coefficients $a = (\gamma_g + 1)\omega_{0g}^2/2v_{0g}$ and $b = 1/6v_{0g}$ are constant. The numerical experiments last a total time T_t . In the following studies, Section 3, the value of this parameter T_t is high enough to ensure that the steady state of the waves is reached. The system is closed by supposing that the liquid and the bubbles are unperturbed at the onset of the studies:

$$p(x \neq 0, 0) = 0,$$

$$v(x, 0) = 0,$$

$$\frac{\partial p}{\partial t}(x \neq 0, 0) = 0, \quad (3)$$

$$\frac{\partial v}{\partial t}(x, 0) = 0, \quad 0 \leq x \leq L,$$

and the resonator is excited by a time-dependent pressure source $s(t)$ placed at $x = 0$:

$$p(x = 0, t) = s(t), \quad 0 \leq t \leq T_t, \quad (4)$$

and a free-wall condition is imposed at the reflector:

$$p(L, t) = 0, \quad 0 \leq t \leq T_t. \quad (5)$$

To solve this differential system, we use a numerical model developed in [24] based on a finite volume method in the space dimension and a finite difference method in the time domain. The frequency components of the time-dependent solution used in the next section are obtained by applying a fast Fourier transform.

3. Results

The objective of this section is, using the phenomenon known as nonlinear frequency shift [22, 28, 29], to show the enhancement of the difference-frequency component generated in a cavity that contains a bubbly liquid by nonlinearly mixing two signals of different frequencies.

The following data for the bubbly liquid are set into the model: $c_{01} = 1500$ m/s, $\rho_{01} = 1000$ kg/m³, and $\nu_1 = 1.43 \times 10^{-6}$ m²/s for the liquid (water) and $c_{0g} = 340$ m/s, $\rho_{0g} = 1.29$ kg/m³, and $\nu_g = 1.4$ for the gas (air). We use bubbles of radius $R_{0g} = 2.5$ μ m, and the bubble density is $N_g = 5 \times 10^{11}$ m⁻³.

Although very few studies exist in the literature, the dependence of the resonance of a bubble cloud on pressure amplitude is a phenomenon, known as nonlinear frequency shift, that has been observed previously in seminal papers by Omta [22], Matsumoto and Yoshizawa [28], and Doc et al. [29]. In Appendix, we show some results obtained with the model described in the above section that corroborate the conclusions of these papers: (i) the increase of pressure amplitude induces the nonlinear frequency shift of the cavity resonance; (ii) this effect relies on the softening of the bubbly liquid, that is due to the variation of the average volume of bubbles; and (iii) this nonlinear effect is more pronounced at higher void fraction in the cavity.

We focus now on the discussion on the application of the softening behavior of the bubbly liquid by taking advantage of the nonlinear frequency shift to strengthen the amplitude of the difference-frequency component generated in the context of the nonlinear frequency mixing of two signals of different frequencies [1, 31]. To this purpose, the analysis is performed by means of a comparison of several numerical experiments for which we search the highest response by parametric emission, i.e., the maximal response of the system at the difference frequency $f_d = f_2 - f_1$: (1) by setting the first primary source frequency f_1 at a constant value and moving the second primary source frequency f_2 , with the same constant source amplitude for both the first and the second primary signals $p_{01} = p_{02}$; (2) by setting f_1 at a constant value and moving f_2 and considering two subcases, (a) a constant p_{02} and a varied p_{01} and (b) a constant p_{01} and a varied p_{02} ; (3) by setting f_2 at a constant value and moving f_1 , with the same constant value $p_{01} = p_{02}$.

To this end, in this section the pressure source we use is $s(t) = p_{01} \sin(\omega_1 t) + p_{02} \sin(\omega_2 t)$, where $\omega_1 = 2\pi f_1$ and $\omega_2 = 2\pi f_2$. The cavity length is set to fit the linear resonance at the difference frequency $f_{dL} = 200$ kHz, $L = \lambda_{dL}/2 = 0.0031$ m, where $\lambda_{dL} = c_{dL}/f_{dL}$ is the wavelength and $c_{dL} = 1222.8$ m/s is the sound speed in this biphasic and dispersive medium at this frequency [3]. We study the nonlinear resonance shift of the difference-frequency component of the signal pressure in the cavity. For each numerical experiment 1 to 3, simulations are performed varying the source amplitude. For each amplitude, we apply a frequency sweep, in such a way that the difference frequency f_d is around the linear resonance f_{dL} , by increments $\delta f = 10$ Hz to evaluate the highest difference-frequency pressure amplitude reached in the cavity p_{dm} at each frequency, and the maximal value p_{dmax} over the frequency range is then localized. Note that we work at primary frequencies chosen to be close to half the resonance frequency of the bubbles since the nonlinearity is high at this frequency in the dispersive medium [3].

Case 1. The first primary frequency is constant, $f_1 = 700$ kHz, whereas the second primary source

frequency f_2 is moved from 896 kHz up to 902 kHz. The source amplitude is varied from $p_{01} = p_{02} = 1$ kPa up to $p_{01} = p_{02} = 6.5$ kPa. Figure 1 shows the result, i.e., p_{dm} as a function of frequency (around f_{dL}) over the amplitude range. It is seen here that the behavior of the difference-frequency component is assimilated to others previously observed through other frequencies, i.e., it shows the same main properties when amplitude is raised as the ones described in the literature and in Appendix [22, 28, 29], which means that the amplitude-dependent behavior of the medium can also be characterized by the behavior of f_d . The resonance of the cavity at the difference frequency clearly undergoes a dependence on pressure amplitude, i.e., a nonlinear frequency shift exists. This means that the softening of the bubbly liquid in the cavity with pressure amplitudes also affects the difference-frequency component. In this case, at $p_{01} = p_{02} = 6.5$ kPa, the resonance is at $f_d = 197.6$ kHz, denoted by f_{dNL} , the frequency shift is $\Delta f_{dNL} = 2.4$ kHz, and the highest value is $p_{dNL} = 19.794$ kPa, which is 304.5% of the source amplitude. Since L is constant, this frequency shift means that the sound speed in the medium is $c_{dNL} = 2L f_{dNL} = 1208.12$ m/s. Also, the symmetry of the curves around the linear resonance observed at the lowest amplitudes is lost when the latest rise, the nonlinear attenuation reduces the ratio of p_{dmax} to source amplitude.

Figure 2 presents the frequency shift Δf obtained as a function of pressure amplitude at the source $p_{01} = p_{02}$ (a), as a function of average bubble volume increase Δv (b), and the maximal value of difference-frequency pressure amplitude reached in the cavity p_{dmax} over the frequency range as a function of pressure amplitude at the source $p_{01} = p_{02}$ (c). The fitting curves are also displayed (green color). A 4th degree polynomial fit is obtained for Figure 2(a). This means that the frequency shift increases hugely as the pressure amplitude rises. The linear dependence of the frequency shift observed in Figure 2(b) proves that the softening of the medium is due to the increase of the mean bubble volume that raises the compressibility, and thus, the nonlinearity of the bubbly medium. Figure 2(c) is a consequence of the two other diagrams, and a 3rd degree polynomial fit is obtained, which means that the nonlinearity of the medium due to the increase of the pressure amplitude generates a huge difference-frequency amplitude.

The source amplitude for this study is $p_{01} = p_{02} = 6.5$ kPa, and we analyze the difference-frequency generation by comparing the results when we do take into account the nonlinear resonance frequency shift and when we do not. The study is thus performed at two difference frequencies, $f_{dL} = 200$ kHz, which is the linear resonance, and $f_{dNL} = 197.6$ kHz, which is the nonlinear resonance found above at this source amplitude (Figure 1), i.e., the frequency that produces the highest response by parametric emission in this case. The primary frequencies at the source are set at $f_{1L} = 700$ kHz and $f_{2L} = f_{1L} + f_{dL} = 900$ kHz for the linear resonance case and at $f_{1NL} = 700$ kHz and $f_{2NL} = f_{1NL} + f_{dNL} = 897.6$ kHz for the nonlinear resonance case. Figure 3 shows the pressure amplitude distribution along the cavity of the primary frequencies f_{1L} , f_{2L} , the difference frequency f_{dL}

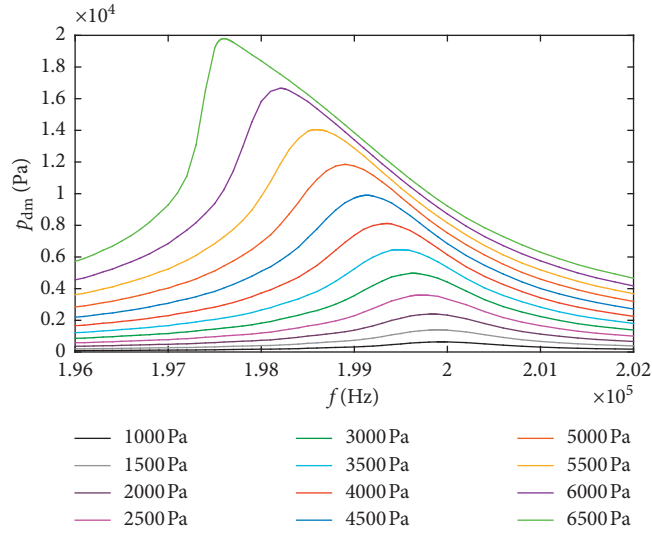


FIGURE 1: Maximum difference-frequency pressure amplitude in the cavity p_{dm} vs. frequency (around f_{dl}) for different source amplitudes in Case 1.

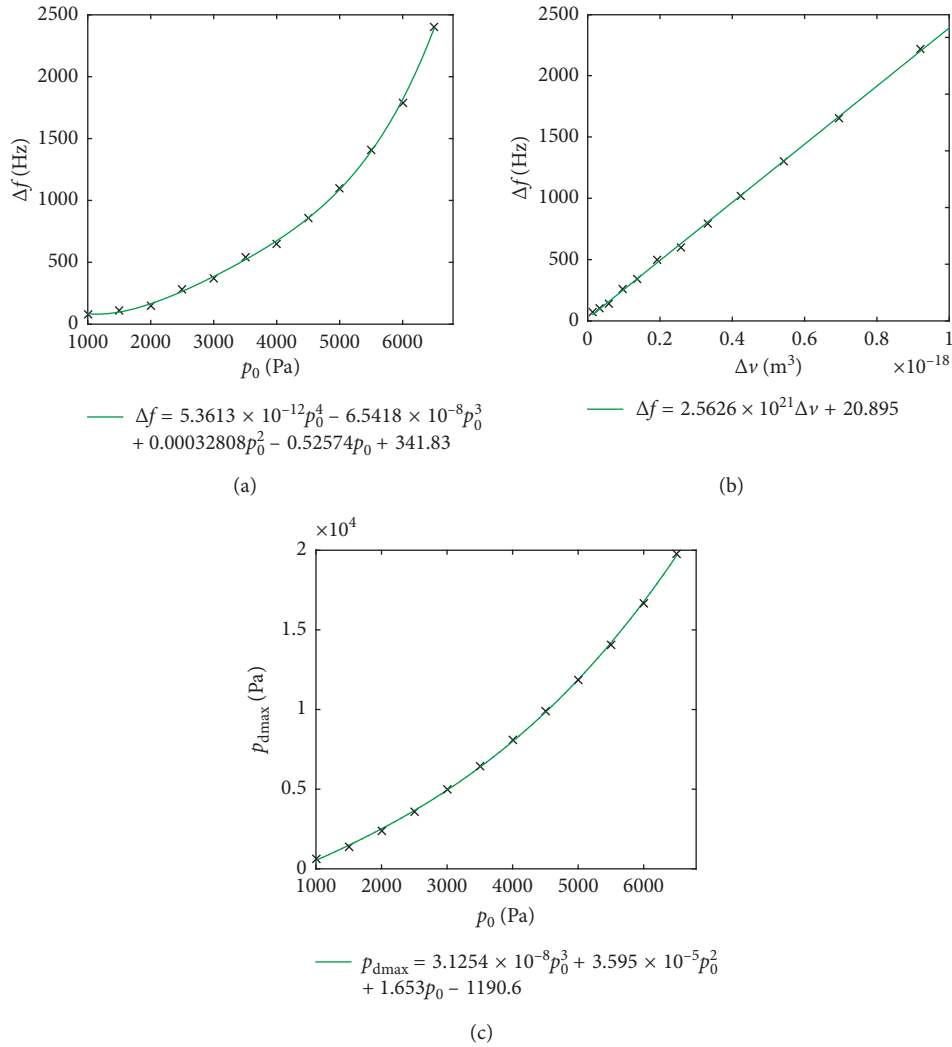


FIGURE 2: Fitting curves in Case 1 of frequency shift Δf vs. pressure amplitude at the source $p_{01} = p_{02}$, denoted by p_0 in (a) and vs. average volume increase Δv (b) and maximal value of difference-frequency pressure amplitude p_{dmax} over the frequency range vs. pressure amplitude at the source $p_{01} = p_{02}$, denoted by p_0 in (c).

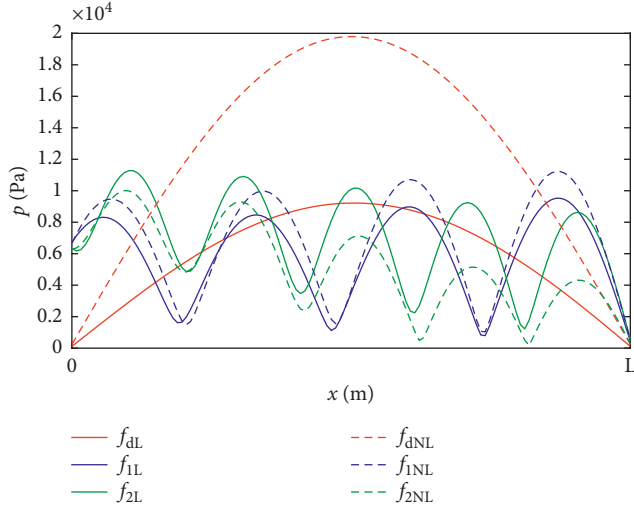


FIGURE 3: Pressure amplitude distribution of frequency components along the resonator in Case 1 at $p_{01} = p_{02} = 6.5$ kPa: $f_{1L} = 700$ kHz, $f_{2L} = 900$ kHz, $f_{dL} = 200$ kHz (blue, green, and red continuous lines, respectively) and $f_{1NL} = 700$ kHz, $f_{2NL} = 897.6$ kHz, $f_{dNL} = 197.6$ kHz (blue, green, and red dashed lines, respectively).

(continuous lines), the primary frequencies f_{1NL} , f_{2NL} , and the difference frequency f_{dNL} (dashed lines). Different amplitudes are observed for f_{dL} and f_{dNL} . The response at the difference frequency is much better by taking into account the nonlinear frequency shift. Whereas the maximum pressure for f_{dL} is $p_{dL} = 9.217$ kPa (141.8% of the source amplitude), the corresponding value for f_{dNL} is $p_{dNL} = 19.794$ kPa (304.5% of the source amplitude, which is a very high value for parametric emission). The benefit drawn in terms of difference-frequency amplitude is 162.7%. It is also interesting to note that by moving one of the primary source frequencies, f_2 from f_{2L} to f_{2NL} , its amplitude decreases, $p_{f_{2NL}} < p_{f_{2L}}$, whereas the amplitude of the other primary signal increases, $p_{f_{1NL}} > p_{f_{1L}}$. This results clearly shows that, by taking into account the resonance frequency shift, the second source frequency is the one that undergoes a strong loss of energy to feed the difference-frequency component that acquires intensity and becomes much stronger, $p_{dNL} > p_{dL}$. This behavior is most likely due to the fact that f_2 is closer to the bubble resonance (see Case 3).

Case 2. The first primary frequency is constant, $f_1 = 700$ kHz, whereas the second primary source frequency f_2 is moved from 896 kHz up to 902 kHz. Two configurations are considered here. For the first one, the source amplitude of the second primary component is constant, $p_{02} = 6.5$ kPa, whereas the source amplitude of the first primary component is varied from $p_{01} = 6.5$ kPa up to $p_{01} = 8.125$ kPa. Figure 4(a) shows p_{dm} as a function of frequency (around f_{dL}) for three amplitude values. At $p_{01} = 8.125$ kPa, the resonance is at $f_{dNL} = 196.54$ kHz, the frequency shift is $\Delta f_{dNL} = 3.46$ kHz, and the highest value is $p_{dNL} = 22.276$ kPa, which is 274.2% of the source amplitude. Since L is constant, this frequency shift means that the sound speed in the medium is $c_{dNL} = 2Lf = 1201.65$ m/s. For the

second configuration, the source amplitude of the first primary component is constant, $p_{01} = 6.5$ kPa, whereas the source amplitude of the second primary component is varied from $p_{02} = 6.5$ kPa up to $p_{02} = 8.125$ kPa. Figure 4(b) shows p_{dm} as a function of frequency (around f_{dL}) for three amplitude values. At $p_{02} = 8.125$ kPa, the resonance is at $f_{dNL} = 196.24$ kHz, the frequency shift is $\Delta f_{dNL} = 3.76$ kHz, and the highest value is $p_{dNL} = 23.674$ kPa, which is 291.4% of the source amplitude. Since L is constant, this frequency shift means that the sound speed in the medium is $c_{dNL} = 2Lf_{dNL} = 1199.81$ m/s.

It must be noted that the nonlinear curves are not symmetric. Also, the maximal values obtained for Case 2 are lower, relatively to the source amplitude (even at more source amplitude), than the one obtained for Case 1, for which the same amplitude at the source is applied to both primary frequencies.

Case 3. The second primary frequency is constant, $f_2 = 900$ kHz, whereas the first primary source frequency f_1 is moved from 698 kHz up to 704 kHz. The source amplitude is set at $p_{01} = p_{02} = 6.5$ kPa. Figure 5 shows the comparison of p_{dm} as a function of frequency (around f_{dL}) over the amplitude range in this case and in Case 1. The general behavior observed in Case 1 becomes apparent here as well, especially a clear nonlinear frequency shift of resonance at the difference frequency compared to the linear resonance. However, the efficiency of the mixing-frequency process is higher in Case 3, giving a higher amplitude of the difference-frequency component, $p_{dNL} = 20.825$ kPa (320.4% of the source amplitude, at $f_{dNL} = 197.38$ kHz with $\Delta f_{dNL} = 2.62$ kHz) instead of $p_{dNL} = 19.794$ kPa (304.5% of the source amplitude, at $f_{dNL} = 197.6$ kHz with $\Delta f_{dNL} = 2.4$ kHz) in Case 1. In Case 3, the sound speed in the medium is $c_{dNL} = 2Lf_{dNL} = 1206.83$ m/s instead of $c_{dNL} = 2Lf_{dNL} = 1208.12$ m/s in Case 1.

This effect is the most likely due to the following. At finite amplitude, the bubble resonance also undergoes a variation from its linear value, $f_{0g} = \omega_{0g}/(2\pi) = 1.34$ MHz, toward lower frequencies, and this frequency shift increases with amplitudes [10]. Thus, when f_2 is constant, at high amplitudes the difference between the nonlinear bubble resonance and the primary frequency f_2 is significantly reduced, whereas when f_1 is constant that difference depends on f_2 that is moving (toward lower values when fitting the nonlinear resonance). Since the primary frequency f_2 is the one that gives most energy to the difference-frequency component [24], the f_2 component of the source then tends to excite the bubbles with more intensity in such a way that the bubbles oscillate around a mean volume that is higher in Case 3 than in Case 1. The softening of the bubbly medium that takes place in the cavity is thus more pronounced in Case 3 than in Case 1 (see Appendix and Refs. [22, 28, 29]), and this gives way to a frequency shift of the difference frequency in the cavity that is higher and produces more intensity in Case 3 than in Case 1.

The results obtained in this section suggest the following new points that are of great interest in the framework of nonlinear ultrasound in bubbly liquids: the nonlinear

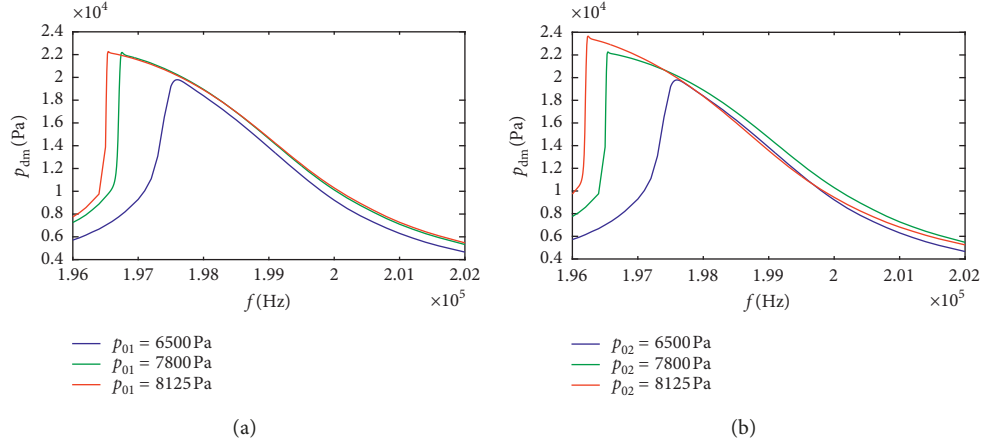


FIGURE 4: Maximum difference-frequency pressure amplitude in the cavity p_{dm} vs. frequency (around f_{dL}) in Case 2 (constant f_1 , varied f_2) for (a) $p_{02} = 6.5$ kPa and three values of p_{01} and (b) $p_{01} = 6.5$ kPa and three values of p_{02} .

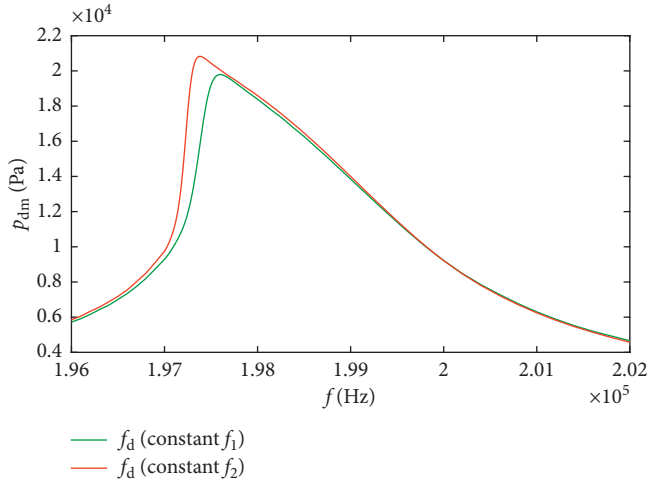


FIGURE 5: Maximum difference-frequency pressure amplitude in the cavity p_{dm} vs. frequency (around f_{dL}) for $p_{01} = p_{02} = 6.5$ kPa in Case 1 (constant f_1 , varied f_2 , green line) and Case 3 (varied f_1 , constant f_2 , red line).

frequency shift of the cavity resonance (decrease of sound speed, softening of the medium by increase of the effective bubble volume with pressure amplitude) can be applied to the mixing of two signals of different frequencies to strengthen the nonlinear generation of the difference frequency component; the comparison of Cases 1 and 2 and Cases 1 and 3 performed above, with primary frequencies well below the bubble resonance, evidences that the enhancement of the difference-frequency component at the nonlinear resonance is very effective (in relation to the source amplitude) when the second primary frequency is constant, whereas the first one is varied to match the nonlinear resonance, and both primary component amplitudes are set at the same value; an unbalanced contribution, in terms of amplitudes, of the primary signals limits the necessary equilibrium to maximize the difference frequency but promotes the generation of harmonics of the strongest primary signal; and a variation of the second primary frequency instead of the first one limits the efficiency of the nonlinear mixing frequency.

4. Conclusions

This work shows that a frequency shift, which grows with pressure amplitudes (nonlinear resonance effect), of a system composed by a bubbly liquid in a cavity exists at the difference-frequency component generated by nonlinear frequency mixing of two primary signals at frequencies well below the bubble resonance. This numerical study also analyzes different ways to enhance the intensity of the difference-frequency signal using this nonlinear resonance effect and suggests the use at the source of a constant second primary frequency combined with a varied first primary frequency to adjust the difference frequency at the nonlinear resonance, both at the same amplitude.

Appendix

In this appendix, we study the nonlinear resonance shift in the cavity for a single-frequency excitation around $f = 200$ kHz with the bubble density $N_{g2} = 5 \times 10^{11} \text{ m}^{-3}$. The pressure source used is $s(t) = p_0 \sin(\omega_f t)$ where p_0 is the amplitude, $\omega_f = 2\pi f$. The length of the cavity is set to be resonant at $L = \lambda/2$, where $\lambda = c_f/f$ is the wavelength and c_f is the sound speed in this biphasic and dispersive medium at this frequency [3]. At $f = 200$ kHz, $c_f = 1222.8$ m/s and $L = c_f/2f = 0.0031$ m. We perform simulations varying p_0 from 1 Pa up to 250 Pa, and at each amplitude, a frequency sweep around f is done (with increment $\delta f = 10$ Hz) to localize the frequency at which the maximum pressure amplitude is reached in the cavity p_m . Figure 6(a) shows the result. For the lowest amplitudes (linear case), the curve is perfectly symmetric, and $p_{\max} = 113 \text{ Pa} = p_L$ corresponds to the linear resonance $f_L = 200$ kHz for $p_0 = 1$ Pa. By increasing p_0 , p_{\max} corresponds to lower frequencies (the nonlinear resonance and the frequency shift are amplitude dependent), and it is also reduced in relation to p_0 due to the nonlinear attenuation, and the symmetry around the resonance is lost. Similitude about the behavior of the frequency shift from the linear resonance with the frequency variation undergone by the single bubble resonance shown by Lauterborn exists [10].

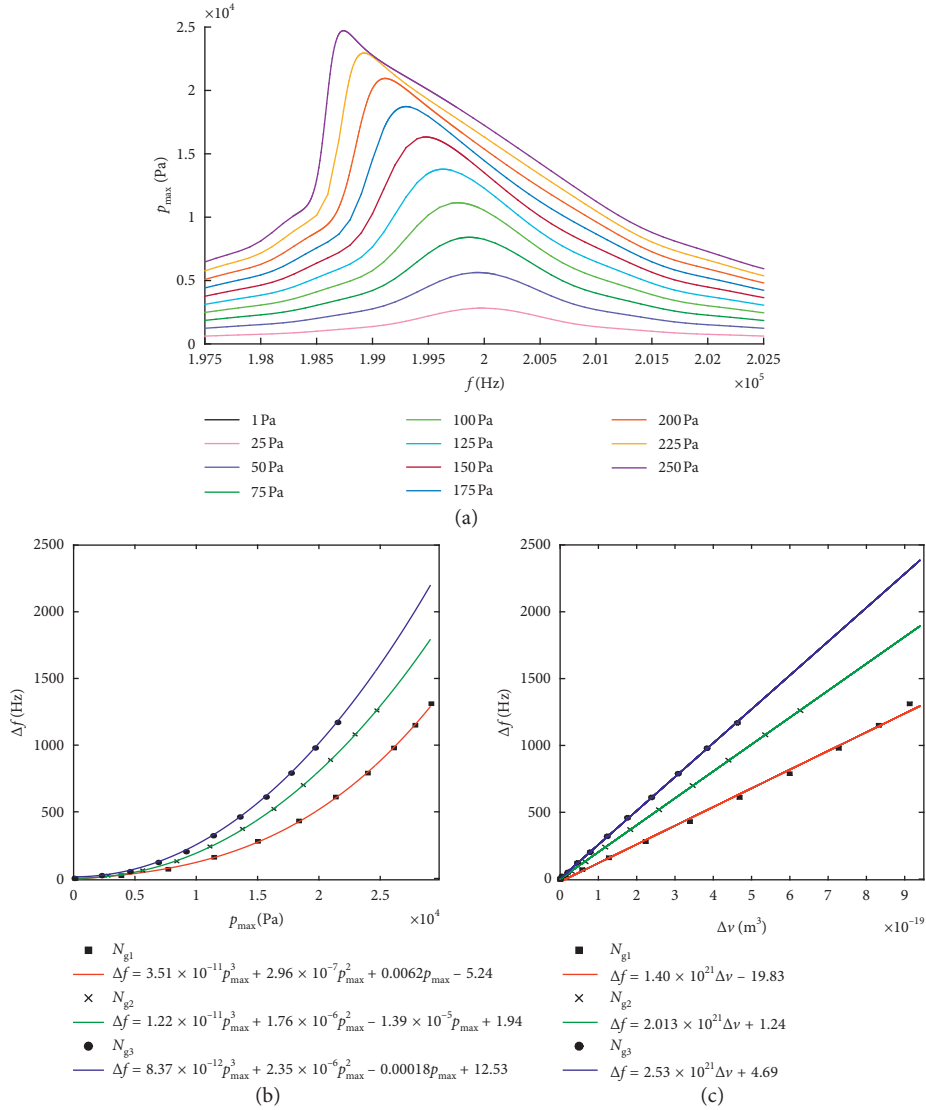


FIGURE 6: Maximum pressure in the cavity p_m vs. source frequency (f) for different source amplitudes p_0 (a); fitting curves of resonance frequency shift Δf vs. pressure amplitude p_{\max} (b) and vs. average volume increase Δv (c), for different bubble densities N_g .

For $p_0 = 250$ Pa, the resonance is at $f_{\text{NL}} = 198.74$ kHz (the frequency shift is $\Delta f_{\text{NL}} = 1.26$ kHz). Since L remains the same at all amplitudes, the resonance shift means a change of sound speed in the medium with amplitudes. This value here is $c_{\text{NL}} = 2Lf_{\text{NL}} = 1215.1$ m/s. Thus, the medium experiences a modification of its acoustic properties when amplitudes change, not only on a local basis (velocity of particles) when nonlinear distortion occurs (e.g., as for a shock wave), but on a global basis. It undergoes a softening process when pressure amplitudes are raised, due to the increase of the effective bubble volume. At nonlinear regime, the positive volume variations prevail over the negative values, and the bubble oscillations are then produced around a mean volume that is bigger than the initial one, $v_{0g}^+ > v_{0g}$, which lowers the sound speed in the effective medium [3]. The effect of the variation of bubble density in the cavity on its nonlinear resonance shift is briefly described in the following. The sound speed and resonator length are $c_f = 1314.1$ m/s and $L = c_f/2f = 0.0033$ m for $N_{g1} = 3 \times 10^{11}$ m^{-3} , $c_f =$

1222.8 m/s and $L = c_f/2f = 0.0031$ m for N_{g2} , and $c_f = 1148.2$ m/s and $L = c_f/2f = 0.0029$ m for $N_{g3} = 7 \times 10^{11}$ m^{-3} . We keep the same amplitude sweeping range as above. Figure 6(b) represents the resonance frequency variation from the linear resonance at $f = 200$ kHz as a function of p_{\max} for each bubble density, including the 3rd degree polynomial fitting of the resonance frequency variation, where Δf is expressed in Hz and p_{\max} in Pa. For the same amplitude, the frequency shift is more pronounced at higher bubble density, since the nonlinear acoustic parameter is higher. Moreover, at constant amplitude, Δf seems to have a pseudolinear behavior vs. bubble density, which is qualitatively coherent with the results given by Brennen [5]. Nevertheless, note that for the same source amplitude, the maximum pressure reached is higher when the bubble density is lower, since there is less attenuation in the medium. Figure 6(c) shows the frequency shift as a function of the average volume increase Δv for each bubble density. The frequency shift increases (higher maximum pressure,

Figure 6(b)) with Δv , i.e., when the effective bubble volume is higher, following a linear fit, where Δf is expressed in Hz and Δv in m^3 . These conclusions are in concordance with other results published in the literature [22, 28], which results in a qualitative validation of our model and procedure.

Data Availability

No data were used to support this study.

Conflicts of Interest

The authors declare that there are no conflicts of interest regarding the publication of this paper.

Acknowledgments

This work was supported by the National Agency for Research (Agencia Estatal de Investigación, AEI), Ministry of Economy, Industry, and Competitiveness of Spain (Ministerio de Economía, Industria y Competitividad), Ministry of Science, Innovation, and Universities of Spain (Ministerio de Ciencia, Innovación y Universidades), and the European Regional Development Fund (FEDER) (grant nos. DPI2012-34613, BES-2013-064399, and DPI2017-84758-P). Christian Vanhille dedicates this work to Dr. Cleofé Campos-Pozuelo.

References

- [1] K. Naugolnykh and L. Ostrovsky, *Nonlinear Wave Processes in Acoustics. Cambridge Texts in Applied Mathematics*, Cambridge University Press, Cambridge, UK, 1998.
- [2] F. Grieser, P. K. Choi, N. Enomoto, H. Harada, K. Okitsu, and K. Yasui, *Sonochemistry and the Acoustic Bubble*, Elsevier Science, Amsterdam, Netherlands, 2015.
- [3] M. F. Hamilton and D. T. Blackstock, *Nonlinear Acoustics*, Academic Press, Cambridge, MA, USA, 1998.
- [4] O. V. Rudenko and S. I. Soluian, *Theoretical Foundations of Nonlinear Acoustics*, Consultants Bureau, New York, NY, USA, 1977.
- [5] C. E. Brennen, *Cavitation and Bubble Dynamics*, Oxford University Press, Oxford, UK, 1995.
- [6] T. J. Mason and J. P. Lorimer, *Applied Sonochemistry: the Uses of Power Ultrasound in Chemistry and Processing*, Wiley-VCH, Weinheim, Germany, 2002.
- [7] Y. Matsumoto, J. S. Allen, S. Yoshizawa, T. Ikeda, and Y. Kaneko, "Medical ultrasound with microbubbles," *Experimental Thermal and Fluid Science*, vol. 29, no. 3, pp. 255–265, 2005.
- [8] O. V. Abramov, *Ultrasound in Liquid and Solid Metals*, CRC Press, Boca Raton, FL, USA, 1994.
- [9] J. A. Gallego-Juárez and K. F. Graff, *Power ultrasonics: Applications of High-Intensity Ultrasound*, Elsevier, Amsterdam, Netherlands, 2014.
- [10] W. Lauterborn, "Numerical investigation of nonlinear oscillations of gas bubbles in liquids," *Journal of the Acoustical Society of America*, vol. 59, no. 2, pp. 283–293, 1976.
- [11] W. Lauterborn, *Nonlinear Acoustics and Acoustic Chaos*, Springer, Berlin, Germany, 2002.
- [12] T. S. Desser and R. B. Jeffrey, "Tissue harmonic imaging techniques: physical principles and clinical applications," *Seminars in Ultrasound, CT and MRI*, vol. 22, no. 1, pp. 1–10, 2001.
- [13] B. N. Kim and S. W. Yoon, "Nonlinear parameter estimation in water-saturated sandy sediment with difference frequency acoustic wave," *Ultrasonics*, vol. 49, no. 4-5, pp. 438–445, 2009.
- [14] D. N. Sinha and C. Pantea, "Broadband unidirectional ultrasound propagation using sonic crystal and nonlinear medium," *Emerging Materials Research*, vol. 2, no. 3, pp. 117–126, 2013.
- [15] V. L. Newhouse and P. Mohana Shankar, "Bubble size measurements using the nonlinear mixing of two frequencies," *Journal of the Acoustical Society of America*, vol. 75, no. 5, pp. 1473–1477, 1984.
- [16] J. C. Buckley, D. A. Knaus, D. L. Alvarenga, M. A. Kenton, and P. J. Magari, "Dual-frequency ultrasound for detecting and sizing bubbles," *Acta Astronautica*, vol. 56, no. 9–12, pp. 1041–1047, 2005.
- [17] M. Cavaro, C. Payan, and J. Moysan, "Microbubble cloud characterization by nonlinear frequency mixing," *Journal of the Acoustical Society of America*, vol. 129, no. 5, pp. EL179–EL183, 2011.
- [18] C. Vanhille, "Two-dimensional numerical simulations of ultrasound in liquids with gas bubble agglomerates: examples of bubbly-liquid-type acoustic metamaterials (BLAMMs)," *Sensors*, vol. 17, no. 12, p. 173, 2017.
- [19] G. Servant, J. P. Caltagirone, A. Gérard, J. L. Laborde, and A. Hita, "Numerical simulation of cavitation bubble dynamics induced by ultrasound waves in a high frequency reactor," *Ultrasonics Sonochemistry*, vol. 7, no. 4, pp. 217–227, 2000.
- [20] S. Dähnke and F. J. Keil, "Modeling of three-dimensional linear pressure fields in sonochemical reactors with homogeneous and inhomogeneous density distributions of cavitation bubbles," *Industrial and Engineering Chemistry Research*, vol. 37, no. 3, pp. 848–864, 1998.
- [21] K. W. Commander and A. Prosperetti, "Linear pressure waves in bubbly liquids: comparison between theory and experiments," *Journal of the Acoustical Society of America*, vol. 85, no. 2, pp. 732–746, 1989.
- [22] R. Omta, "Oscillations of a cloud of bubbles of small and not so small amplitude," *Journal of the Acoustical Society of America*, vol. 82, no. 3, pp. 1018–1033, 1987.
- [23] C. Vanhille and C. Campos-Pozuelo, "Numerical simulation of nonlinear ultrasonic standing waves in bubbly liquid," *International Journal of Nonlinear Sciences and Numerical Simulation*, vol. 10, no. 6, pp. 751–757, 2009.
- [24] M. T. Tejedor Sastre and C. Vanhille, "A numerical model for the study of the difference frequency generated from nonlinear mixing of standing ultrasonic waves in bubbly liquids," *Ultrasonics Sonochemistry*, vol. 34, pp. 881–888, 2017.
- [25] U. Polimeno and M. Meo, "Detecting barely visible impact damage detection on aircraft composites structures," *Composite Structures*, vol. 91, no. 4, pp. 398–402, 2009.
- [26] P. A. Johnson and X. Jia, "Nonlinear dynamics, granular media and dynamic earthquake triggering," *Nature*, vol. 437, no. 7060, pp. 871–874, 2005.
- [27] M. P. Mortel and B. R. Seymour, "Nonlinear resonant oscillations in closed tubes of variable cross-section," *Journal of Fluid Mechanics*, vol. 519, pp. 183–199, 2004.
- [28] Y. Matsumoto and S. Yoshizawa, "Behaviour of a bubble cluster in an ultrasound field," *International Journal for Numerical Methods in Fluids*, vol. 47, no. 6-7, pp. 591–601, 2005.

- [29] J.-B. Doc, J.-M. Conoir, R. Marchiano, and D. Fuster, "Nonlinear acoustic propagation in bubbly liquids: multiple scattering, softening and hardening phenomena," *Journal of the Acoustical Society of America*, vol. 139, no. 4, pp. 1703–1712, 2016.
- [30] E. A. Zabolotskaya and S. I. Soluyan, "Emission of harmonic and combination-frequency waves by bubbles," *Acoustical Physics*, vol. 18, no. 3, pp. 396–398, 1973.
- [31] S. Karpov, A. Prosperetti, and L. Ostrovsky, "Nonlinear wave interactions in bubble layers," *Journal of the Acoustical Society of America*, vol. 113, no. 3, pp. 1304–1316, 2003.



Hindawi

Submit your manuscripts at
www.hindawi.com

